



Cavitation to fracture transition in a soft solid

Cite this: DOI: 10.1039/c7sm01479a

Jingtian Kang,^{ab} Changguo Wang^{*b} and Shengqiang Cai^{id} ^{*a}

Received 26th July 2017,
 Accepted 19th August 2017

DOI: 10.1039/c7sm01479a

rsc.li/soft-matter-journal

When a soft solid such as rubber, gel and soft tissue is subject to hydrostatic tension, a small cavity inside the solid expands. For a neo-Hookean solid, when the hydrostatic tension approaches a critical value: 2.5 times its shear modulus, the initially small cavity can expand unboundedly. Such a phenomenon is usually referred to as cavitation instability in soft solids. Several recent experiments have shown that fractures may occur in the material when the hydrostatic tension is far below the critical value. In this article, we study a spherical cavity with a ring crack on its wall and inside a neo-Hookean elastomer subject to hydrostatic tension. We compute the energy release rate associated with the extension of the ring crack, for both pressure-control and (cavity) volume-control loading modes. We find that for the pressure-control mode, the energy release rate increases with the increase of the crack size as well as the magnitude of pressure; for the (cavity) volume-control mode, with a fixed cavity volume, the energy release rate increases with the increase of the crack size when the crack is short; the energy release rate maximizes for an intermediate crack size, and decreases with the increase of crack size when the crack is long. The results obtained in this article may be helpful for understanding cavitation-to-fracture transition in soft solids subject to different loading conditions.

1. Introduction

When a soft solid is subject to hydrostatic tension, a small cavity initially inside the material expands. Based on the model of assuming a small spherical cavity inside an infinitely large neo-Hookean solid, we can predict that when the hydrostatic tension is small, the cavity expands slowly with increase of hydrostatic tension. When the hydrostatic tension approaches 2.5 times its shear modulus, the cavity expands dramatically with a tiny increase of external stress. Such a phenomenon is usually referred as cavitation instability in elastomeric solids. Pioneering experiments and theoretical analysis done by Gent¹ have quantitatively validated the above prediction for vulcanized rubber. Similar experiments have been recently conducted by Hamdi *et al.*² on styrene butadiene rubber. Making use of cavitation instability in soft solids, Zimmerlin *et al.*^{3,4} developed the cavitation rheology technique to measure the local shear modulus of hydrogels and soft tissues such as brain tissue and bone marrow.⁵

It has been shown in recent experiments which were elegantly done by Poulain *et al.*⁶ that fracturing may occur in the elastomer far before the hydrostatic tension reaching 2.5 times its shear modulus. It has also been shown that because of the

large deformation, cavity expansion cannot be easily distinguished from crack extension.

To study fracture during the cavitating process, William and Schapery⁷ regarded the expansion of a cavity in an elastomer as the process of creating new spherical surface and computed the energy release rate of this process. They obtained the energy release rate of the cavitating process in an elastomer as: $G = \mu R(2\lambda^2 + \lambda^{-4} - 3)$, where R is the initial cavity radius, and λ is the ratio between the radius of the cavity after and before deformation. When the energy release rate is equal to the fracture toughness of the material, cavitation-induced-fracture occurs. In addition to the spherical shape, defects in a solid may have different shapes. Gent and Wang (GW),⁸ and later Lin and Hui (LH),⁹ have calculated the energy release rate in an elastomer with a penny-shape defect, when the elastomer is subject to hydrostatic tension. Using the elastic cavitation results obtained earlier, GW gave the energy release rate as: $G = 2\mu R(1 + \lambda^2 - 2\lambda^{-1})$. It was later pointed out by Lin and Hui that GW overestimated the energy release rate.⁹ LH provided an approximate analytical equation to estimate the energy release rate for an incompressible neo-Hookean material as $G \approx \frac{4\mu R}{3\pi} \left(2\lambda^2 + \frac{1}{\lambda^4} - 3 \right)$. The above equation has shown to be a good approximation to the energy release rate computed by finite element simulations, when the hydrostatic tension is less than 90% of the shear modulus of the elastomer. In addition to the work discussed above, Hutchens *et al.*¹⁰ have recently constructed a mechanism map for the cavitation rheology test considering both elastic deformation and fracture.

^a Department of Mechanical and Aerospace Engineering, University of California, San Diego, La Jolla, CA 92093, USA. E-mail: shqcai@ucsd.edu

^b Center for Composite Material and Structure, Harbin Institute of Technology, Harbin 50001, China. E-mail: wangcg@hit.edu.cn

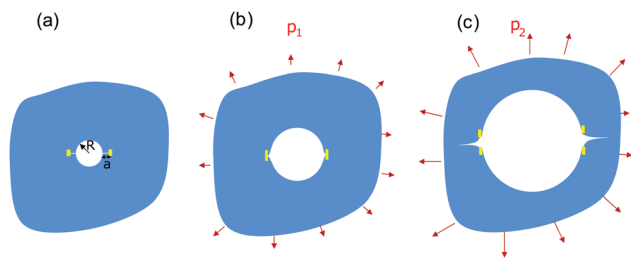


Fig. 1 Schematics of the model for studying cavitation-to-fracture transition in an elastomer subject to externally applied hydrostatic tension. (a) In the undeformed state, a spherical cavity with a ring crack is in the elastomer. (b) When externally applied hydrostatic tension is small, the cavity expands without crack propagation. (c) When the hydrostatic tension is large enough, the crack grows with cavity expansion.

In this article, to study cavitation-to-fracture transition in a soft solid, we reconsider the problem by assuming a spherical cavity inside a soft solid with an edge crack of ring-shape on the cavity wall as shown in Fig. 1. The introduction of an edge crack enables us to study the energy release rate with a clearly defined fracturing surface. When the edge crack is small, it can be regarded as a tiny defect on the cavity wall or small deviations of the cavity from the perfect spherical shape. It has been shown that when rubber blocks are supersaturated with high-pressure dissolved gases or liquids, cavities of spherical shape can often be found in the interior.¹¹ When the size of the edge crack is much bigger than the cavity radius, the introduced defect is similar to a penny-shaped crack in the material. We use finite element simulation to compute the energy release rate of the edge crack for different levels of hydrostatic tension or different volumes of the cavity. We can predict the critical pressure or volume of the cavity for the edge crack to grow if the fracture toughness of the material is known. Our calculations also show that depending on the loading condition, the crack may grow either in a stable or unstable manner.

2. Numerical models

Fig. 1 shows the schematics of our model of studying the cavitation-to-fracture transition in an elastomer subject to external hydrostatic tension. Following most previous work on cavitation in soft solids,^{8,9} we assume a small spherical cavity exists inside the material before the mechanical load is applied. In addition, a pre-existing ring crack is introduced on the cavity wall as shown in Fig. 1a. When the external hydrostatic tension is small, the cavity expands and the wall of the cavity stretches without crack extension as shown in Fig. 1b. When the hydrostatic tension is high enough, the crack extends with cavity expansion (Fig. 1c). It is noted that in the current study, we ignore the interaction among cavities. In another word, we assume the cavities are sparsely distributed in the material, which is also a commonly-adopted assumption in most previous studies.^{3–10}

To calculate the deformation of the elastomer with a cavity and the energy release rate for the crack extension, we use commercially available finite element codes, ABAQUS standard,¹²

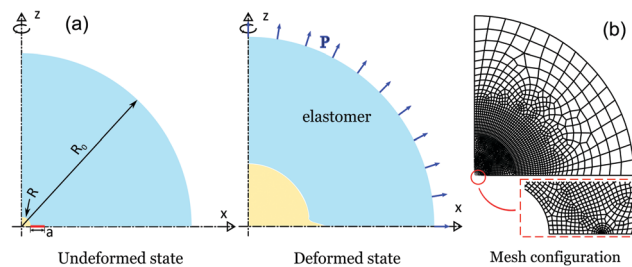


Fig. 2 Schematics of finite element model for calculating energy release rate associated with the growth of the ring crack in the cavitating process. (a) In the undeformed state, a small spherical cavity with radius R is introduced onto the cavity wall. When hydrostatic tension is applied onto the external surface of the elastomer, the cavity expands. Mesh configuration of the finite element model is shown in (b). In the vicinity of the cavity wall and ring crack tip, meshes are greatly refined.

to conduct implicit quasi-static simulations. In the finite element model as shown in Fig. 2, taking advantage of the geometrical symmetry, we only simulate a quarter of a spherical elastomer. In the undeformed state, the radius of the spherical cavity is R and the size of the ring crack is denoted by a . The ratio between the outer radius of the elastomer R_0 and the radius of the cavity R is set to be 200. In the deformed state, external pressure is applied onto the surface of the elastomer, which induces the expansion of the cavity. Mesh configuration of the finite element model is shown in Fig. 2b. The mesh is greatly refined near the cavity. The type of element for the simulation is CAX8H. The total number of elements in the finite element model is 156 528. The incompressible neo-Hookean hyperelasticity model is assigned to the material. The energy release rate is calculated by exporting the J-integral around the crack tip using the contour integral function embedded in ABAQUS. The convergence of the results is guaranteed by checking the independence of the J-integral on different contours around the crack tip.

Based on the finite element simulations, we present the results of the energy release rate for two different loading modes: first, the energy release rate is plotted as a function of crack size with different magnitudes of the external tension; second, the energy release rate is plotted as a function of crack size for different volumes of the cavity.

3. Results and discussions

A spherical cavity inside an infinitely large incompressible neo-Hookean solid expands when the solid is subject to external hydrostatic tension. The relationship between the size of the cavity and the magnitude of the hydrostatic tension is given by,¹

$$P = \mu(5 - 4\lambda^{-1} - \lambda^{-4})/2, \quad (1)$$

where λ is the ratio between the radius of the cavity after and before deformation, and μ denotes the small-deformation shear modulus of the neo-Hookean solid. It can be easily seen from eqn (1) that when the applied pressure approaches 2.5μ , the size of the cavity grows unboundedly. Consequently, the stretch

on the cavity wall can be large enough to induce fracture in the material. It can also be seen from eqn (1) that the critical pressure is independent of the initial cavity size. However, it has been shown in some experiments that a smaller cavity needs larger pressure to grow to visible bubbles,⁷ which indicates the involvement of the fracture during the cavitating process. It is known that the fracture provides an intrinsic length scale: Γ/μ , where Γ is the fracture toughness of the material.

In this article, we consider a cavity with a small ring crack embedded inside an elastomer as shown in Fig. 1. For the pressure-control mode, external hydrostatic tension is applied onto the outer boundary of the elastomer. The energy release rate calculated as a function of pressure is shown in Fig. 3 for different initial ring crack sizes. It is noted that the externally applied hydrostatic tension is equivalent to the application of inflated pressure inside the cavity with the same magnitude, due to the incompressibility of the material. It can be clearly seen from Fig. 3 that with the increase of pressure and the size of the ring crack, the energy release rate increases. When the pressure approaches 2.5 times the shear modulus, the energy release rate increases unboundedly. For comparison, we also plot the results from WS⁷ and from LH⁹ in Fig. 3. When the ring crack is much larger than the cavity, we can recover the results of the energy release rate of a penny-shape defect in an elastomer subject to hydrostatic tension as given by LH.

When $a/(R+a)$ in Fig. 1a is much smaller than one, the ring crack can be viewed as an edge crack with length a in a rectangular elastomer strip, as shown in Fig. 4a. Based on simple scaling analysis, the energy release rate can be given by,

$$G = 2\kappa(\lambda)w(\lambda)a, \quad (2)$$

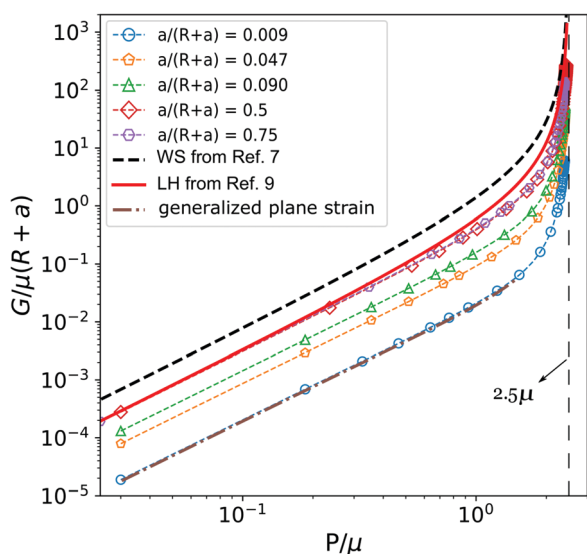


Fig. 3 Dependence of normalized energy release rate on the magnitude of hydrostatic tension for different sizes of the ring crack. When the ring crack is much larger than the cavity radius, we can recover the energy release rate for a penny-shape defect in an elastomer subject to hydrostatic tension. When the ring crack is much smaller than the cavity radius, the ring crack can be viewed as a crack in a rectangular strip.

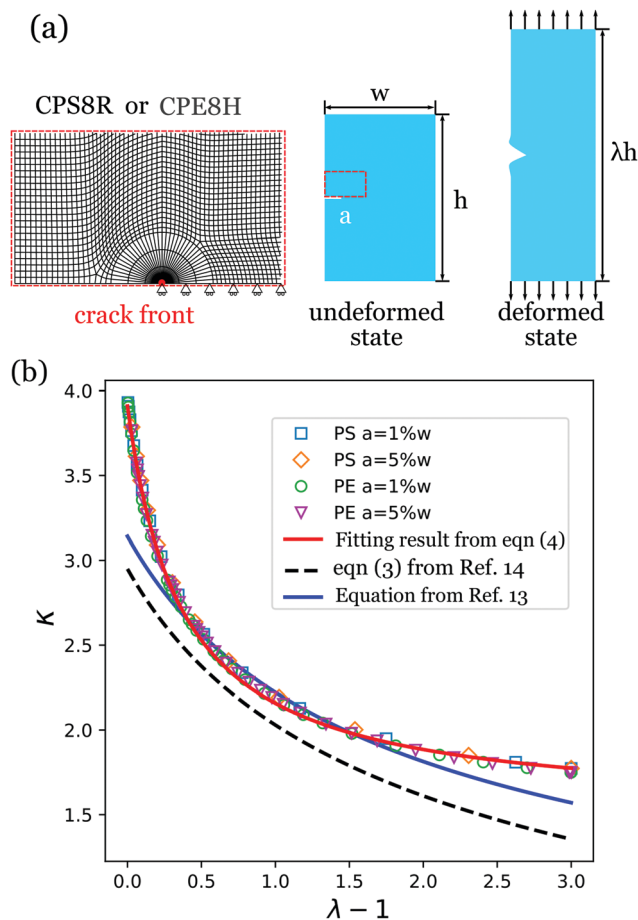


Fig. 4 Finite element computation of the energy release rate of a rectangular neo-Hookean strip with an edge crack and subject to axial stretch. The strip is subject to simple extension or axial stretch under plan strain extension. (a) Schematics of the finite element model. In the undeformed state, the width of the strip is w , its height $h = 4w$, and the length of the edge crack is set to be $a = 1\%w$ and $5\%w$. The element type in the simulation is CPS8R or CPE8H for the plane stress condition and plane strain condition, respectively. (b) The dependence of the dimensionless function $\kappa(\lambda)$ on the axial stretch. $\kappa(\lambda)$ is defined in eqn (2).

where $w(\lambda)$ is the strain energy density of the rectangular elastomer without a crack, yet with the same stretched state, $\kappa(\lambda)$ is a dimensionless function only depending on the stretch state, and a is the size of the edge crack.

For a rectangular elastomer strip subject to simple extension with stretch λ , several different forms of $\kappa(\lambda)$ have been given by different researchers under plane stress conditions. For example, for a central crack in a rectangular thin rubber sheet subject to simple extension, Lake¹³ gave an expression for $\kappa(\lambda)$ as $\kappa(\lambda) = \pi/\sqrt{\lambda}$. Another fitting form of $\kappa(\lambda)$ which has been more widely used is given by Lindley¹⁴ as,

$$\kappa = \frac{2.95 - 0.08\varepsilon}{(1 + \varepsilon)^{1/2}}, \quad (3)$$

where the engineering strain $\varepsilon = \lambda - 1$. It has been pointed out by Yeoh,¹⁵ when the strain is small, the above equation deviates from the prediction from linear fracture mechanics.

To obtain a more accurate formula for the energy release rate, we conduct finite element simulations on a rectangular hyperelastic strip as shown in Fig. 4a. In the undeformed state, the width of the strip is w , and its height is $h = 4w$. Due to the symmetry, only half of the strip is modeled. The length of the edge crack is taken to be $a = 1\%w$ and $5\%w$, respectively. In the deformed state, axial displacement is imposed on its edge as shown in Fig. 4a. We calculate the deformation of the rectangular strip under plane stress and plane strain conditions using CPS8R and CPE8H elements, respectively. The mesh is greatly refined near the crack tip as shown in Fig. 4a. The total number of the elements is 86 260. The material is set to be an incompressible neo-Hookean solid. We calculate the energy release rate by exporting the J-integral around the crack tip using the embedded function of ABAQUS. Based on the numerical results, we propose the following fitting equation for $\kappa(\lambda)$ as defined in eqn (2):

$$\kappa(\lambda) = \frac{1.513\lambda - 0.076}{\lambda - 0.6325}. \quad (4)$$

The fitting result given by eqn (4) is plotted with finite element simulation results in Fig. 4b. When $\lambda \rightarrow 1$, $\kappa \rightarrow 3.9102$ as given by eqn (4), which agrees well with the prediction from linear fracture mechanics.¹⁶ The results in Fig. 4b show that the above equation gives improved predictions for the λ ranging from 1 to 4.

According to our knowledge, for a rectangular elastomer strip with an edge crack and subject to finite axial stretch under plane strain conditions, $\kappa(\lambda)$ is not available in the literature. When the deformation is small, it can be easily shown that the form of $\kappa(\lambda)$ for axial stretch is the same for plane strain condition and plane stress condition. Using finite element simulation, we confirm that finite deformation, $\kappa(\lambda)$ for axial stretch is still the same for plane strain and plane stress conditions as shown in Fig. 4b, by changing $w(\lambda)$ in eqn (2) from axial stretch with plane stress condition to plane strain condition.

The stretch state near the wall of the cavity can be viewed as a generalized plane strain condition. It has been shown that the strain energy state of a deformed hyperelastic material under generalized plane conditions can be directly obtained from the energy obtained under plane strain conditions.¹⁷ The stretch state of the cavity wall can be given by $\lambda_1 = \lambda_2 = \lambda$ and $\lambda_3 = \lambda^{-2}$. As a result, the energy release rate can be given by:

$$G = \frac{2a}{\lambda} \kappa(\lambda_1') w(\lambda_1'), \quad (5)$$

where $\lambda_1' = \lambda\sqrt{\lambda}$, $w(\lambda_1') = \mu(\lambda_1'^2 + \lambda_1'^{-2} - 2)/2$, and $\kappa(\lambda_1')$ can be given by the fitting formula (eqn (4)). A combination of eqn (1) and (5) enables us to obtain the relationship between the energy release rate and the magnitude of the pressure when the crack size is small as shown in Fig. 3. The prediction given by eqn (5) also agrees well with our FEM simulations.

In the experiment of needle-induced cavitation done by Zimmerlin *et al.*,¹⁸ water is continuously injected into an elastomer to induce cavitation. The space of the cavity is completely filled with nearly incompressible water. Therefore, if the water injection

is very slow or quasi-static, the cavitating process in the elastomer can be viewed as a volume-control process.

Motivated by the needle-induced cavitation experiment, we plot the energy release rate as a function of the size of the ring crack for different volumes of the cavity in Fig. 5. With a fixed volume of the cavity, the energy release rate increases with the increase of crack size when the crack is short. The energy release rate maximizes when the crack is of an intermediate length. The energy release rate decreases with further increase of the crack size when the crack is large. The peak values of the energy release rate for different volumes of the cavity are connected by a dashed curve in Fig. 5. According to fracture mechanics, when the energy release rate is equal to or larger than the fracture toughness of the material, the crack begins to grow. Such growth may be either stable or unstable. As we can see from Fig. 5, for a fixed crack length, the energy release rate increases with the increase of the volume of the cavity. Consequently, with a certain initial crack size and fracture toughness of the material, the crack begins to grow when the volume of the cavity increases to a critical value. If the initial ring crack is small, namely on the left of the dashed curve in Fig. 5, with a fixed volume of the cavity, the energy release rate first increases and then decreases with the increase of crack size. This indicates that the crack may grow unstably first and then be arrested when the energy release rate is equal to the fracture toughness of the material again as shown in the horizontal dash line in Fig. 5. Such unstable crack growth may induce a drop of pressure of the water. If the initial ring crack is large, namely on the right of the

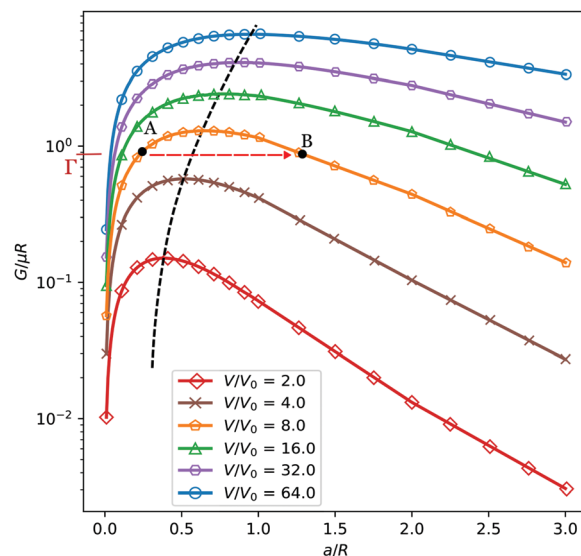


Fig. 5 The dependence of normalized energy release rate on the size of ring crack for different volumes of the cavity. V_0 is the initial cavity volume in the undeformed elastomer, V is the cavity volume after deformation. The black dashed curve connects the peak values for different volumes of the cavity. If the initial ring crack size is small (left side of the curve) and fracture toughness of the material is Γ (point A in the plot), when the volume of the cavity is large enough ($V/V_0 = 8$), the ring crack will grow unstably from point A to point B with a much larger crack size. The crack is then arrested, and further growth of crack requires increase of the volume of the cavity.

dashed curve in Fig. 5, with a fixed volume of cavity, the energy release rate always decreases with increase of crack size. This indicates that the crack should grow stably when the volume of cavity is large enough, namely, any additional growth of the crack requires increase of the volume of the cavity.

Finally, we would like to note that the results obtained in this article are based on a simplified geometry, *i.e.* a ring crack on the wall of a spherical cavity which is embedded in an infinitely large elastomer. Due to the cavitating process in soft solids, cavities of complex shapes and multiple cracks may exist. Additionally, the loading conditions may be different from both the pressure-control and volume-control model.

4. Concluding remarks

In this article, we study the fracture of an elastomer during the cavitating process. Using the finite element method, we calculate the energy release rate of an elastomer with a spherical cavity and a ring crack on its wall, when subject to hydrostatic tension. Depending on the loading mode and initial ring crack size, the crack may grow stably or unstably during the loading process. The results presented in the article are helpful for understanding the cavitating process in an elastomer and utilizing cavitation rheology to measure the fracture properties of soft solids.

Conflicts of interest

There are no conflicts of interest to declare.

Acknowledgements

S. Cai acknowledges the support from ONR [grant number N00014-17-1-2056]. C. Wang acknowledges financial supports from the National Natural Science Foundation of China, 11572099; the Natural Science Foundation of Heilongjiang Province of China, A2015002; the Fundamental Research Funds for the Central

Universities, HIT.BRETHIII.201209 and HIT.MKSTISP.2016 29; the Aeronautical Science Foundation of China, 2016ZA77001.

References

- 1 A. N. Gent and P. B. Lindley, *Proc. R. Soc. London, Ser. A*, 1959, **249**, 195.
- 2 A. Hamdi, S. Guessasma and M. Nat Abdelaziz, *Mater. Des.*, 2014, **53**, 497–503.
- 3 J. A. Zimmerman, N. Sanabria-DeLong, G. N. Tew and A. J. Crosby, *Soft Matter*, 2007, **3**, 763–767.
- 4 J. A. Zimmerman, J. J. McManus and A. J. Crosby, *Soft Matter*, 2010, **6**, 3632–3635.
- 5 L. E. Jansen, N. P. Birch, J. D. Schiffman, A. J. Crosby and S. R. Peyton, *J. Mech. Behav. Biomed. Mater.*, 2015, **50**, 299–307.
- 6 X. Poulain, V. Lefèvre, O. Lopez-Pamies and K. Ravi-Chandar, *Int. J. Fract.*, 2017, **205**, 1–21.
- 7 M. L. Williams and R. A. Schapery, *Int. J. Fract.*, 1965, **1**, 64–72.
- 8 A. N. Gent and C. Wang, *J. Mater. Sci.*, 1991, **26**, 3392–3395.
- 9 Y. Y. Lin and C. Y. Hui, *Int. J. Fract.*, 2004, **126**, 205–221.
- 10 S. B. Hutchens, S. Fakhouri and A. J. Crosby, *Soft Matter*, 2016, **12**, 2557–2566.
- 11 A. N. Gent, *Rubber Chem. Technol.*, 1990, **63**, 49–53.
- 12 Abaqus Analysis User's Manual. Abaqus 6.12, Dassault Systèmes.
- 13 G. J. Lake, *Int. Conf. Yield, Deformation and Fracture of Polymers*, 1970, p. 47.
- 14 P. B. Lindley, *J. Strain Anal.*, 1972, **7**, 132–140.
- 15 O. H. Yeoh, *Mech. Mater.*, 2002, **34**, 459–474.
- 16 T. L. Anderson, *Fracture mechanics: fundamentals and applications*, CRC Press, 2017.
- 17 W. Hong, X. Zhao and Z. Suo, *Appl. Phys. Lett.*, 2009, **95**, 111901.
- 18 J. A. Zimmerman and A. J. Crosby, *J. Polym. Sci., Part B: Polym. Phys.*, 2010, **48**, 1423–1427.